International Journal of Sediment Research xxx (xxxx) xxx



Contents lists available at ScienceDirect

International Journal of Sediment Research

journal homepage: www.elsevier.com/locate/ijsrc



Original Research

Experimental investigation of the effects of shrub filter strips on debris flow trapping and interception

Songtang He ^{a, b, c, 1}, Wenle Chen ^{d, 1}, Daojie Wang ^{a, b, **}, Xiaoqing Chen ^{a, b, *}, Yuchao Qi ^{a, b, c}, Peng Zhao ^{a, b, c}, Yong Li ^{a, b}, Yongming Lin ^e, Ali Akbar Jamali ^f

- ^a Key Laboratory of Mountain Hazards and Earth Surface Processes, Chinese Academy of Sciences, Chengdu 610041, China
- ^b Institute of Mountain Hazards and Environment, Chinese Academy of Sciences, Chengdu 610041, China
- ^c University of Chinese Academy of Sciences, Beijing 100049, China
- ^d Pipe China Southwest Pipeline Company, Chengdu 610095, China
- e Key Laboratory for Forest Ecosystem Process and Management, College of Forestry, Fujian Agriculture and Forestry University, Fuzhou, 350002, China
- f Department of GIS-RS and Watershed Management, Maybod Branch, Islamic Azad University, Maybod, Yazd, Iran

ARTICLE INFO

Article history: Received 24 November 2021 Received in revised form 2 September 2022 Accepted 14 September 2022 Available online xxx

Keywords: Ecological engineering Mountain hazards mitigation and prevention Shrub filter strips Debris flow Sediment trapping

ABSTRACT

Ecological engineering plays an increasingly significant role in mountain hazard control, but the effect of species selection and arrangement (e.g., row spacing and stem spacing) on debris flow suppression is still unclear. To further understand the interception efficiency of shrub arrangement parameters on debris flow and explore the difference with slow hydraulic erosion, sixteen sets of small-scale flume experiments with different stem and row spacings were done to study the effects of shrubs on debris flow severity, flow rate, velocity, and particle size. The results suggest that, for a dilute debris flow, sediment interception effectiveness (27.4%-60.9%) decreases gradually as stem spacing increases. Moreover, as row spacing increases, flow velocity reduction (34,4%-44.9%) and flow reduction (18,5%-47.4%) gradually decrease; and the bulk density reduction (0.5%-5.3%) and sediment interception increase initially and then decrease. In contrast, for a viscous debris flow, the flow reduction, flow velocity reduction, and sedimentation interception decrease gradually as the stem spacing increases. As row spacing increases, the flow velocity reduction, flow reduction, and sediment interception all increase initially and then decrease. A formula for the flow velocity of dilute debris flow after the filter strip was derived based on the energy conservation law and Bernoulli's equation, confirming that debris flow movement is closely related to the degree of vegetation cover. This research strengthens the current understanding of the effectiveness of vegetation in debris flow disaster prevention and control and can guide practical applications.

© 2022 Published by Elsevier B.V. on behalf of International Research and Training Centre on Erosion and Sedimentation/the World Association for Sedimentation and Erosion Research.

1. Introduction

The debris flow process generally includes initiation, transport, and deposition, among which transport is an important link (Pudasaini & Mergili, 2019). Further, the transport capacity is influenced by the properties of the fluid (components of the particles, viscosity or level of dilution), the underlying surface condition (roughness, slope, distance, and topography; He et al., 2018; Li et al., 2015), and the characteristics of intercepting structures (ecological and geotechnical engineering; Lan et al., 2020; Michelini et al., 2016). Considerable research on sediment transport capacity refers to the fluid characteristics of debris flow (Liu et al., 2020; Yin et al., 2021) and surface condition (Gregoretti & Fontana, 2008) as well as civil engineering features (Sun et al., 2018, 2021). Especially, such geotechnical engineering projects are limited by their design requirements and high costs, which makes them difficult to apply over large areas. The implementation also is challenging in areas with complex or steep terrain, and the

https://doi.org/10.1016/j.ijsrc.2022.09.005

1001-6279/© 2022 Published by Elsevier B.V. on behalf of International Research and Training Centre on Erosion and Sedimentation/the World Association for Sedimentation

Please cite this article as: He, S et al., Experimental investigation of the effects of shrub filter strips on debris flow trapping and interception, International Journal of Sediment Research, https://doi.org/10.1016/j.ijsrc.2022.09.005

^{*} Corresponding author. Key Laboratory of Mountain Hazards and Earth Surface Processes, Chinese Academy of Sciences, Chengdu 610041, China.

^{**} Corresponding author. Key Laboratory of Mountain Hazards and Earth Surface Processes, Chinese Academy of Sciences, Chengdu 610041, China.

E-mail addresses: wangdj@imde.ac.cn (D. Wang), xqchen@imde.ac.cn (X. Chen). These authors contributed equally to this work and should be considered co-

first authors

success of the project cannot be guaranteed. In scenic locations (such as Jiuzhaigou World Natural and Cultural Heritage National Park, China (Hu et al., 2019)), the landscape is fragile and sensitive, and construction can have a significant effect on the environment (Nilsson et al., 2005). In addition, common engineering materials such as steel rebar and concrete are incompatible with the environment, and they can reduce the aesthetic value of areas with natural beauty (Bischetti et al., 2012).

In contrast, there are several advantages of ecological engineering measures, such as self-repairing, long-lasting, low energy consumption, low material consumption, and environmentally compatible (Evette et al., 2009; Stokes et al., 2014). Thus, ecological engineering techniques address the apparent contradiction between preventative engineering methods and environmental protection, and they can even improve mountainous environments while controlling disasters (He et al., 2017). Consequently, the use of vegetation to prevent and mitigate debris-flow disasters is attracting increasing attention (Vargas-Luna et al., 2016; Wang et al., 2018).

Vegetation can act as a physical barrier, altering the sediment flow at the soil surface (Lee et al., 2000; Martinez-Raya et al., 2006). At present, a few researchers have evaluated the influence of stem basal cover, plant communities, slope gradient, and discharge on overland flow to predict transport capacity through experiments and physics-based modeling (Mergili et al., 2020; Mu et al., 2019; Tisserant et al., 2020). Most of the studies have concentrated on general soil and water conservation. However, debris flow is one of the tensive gravitational erosion hazards with high speed and energy (Cui et al., 2019a; Pudasaini, 2012; Pudasaini & Krautblatter, 2021). It is unclear whether the water-interception principle can be applied to vegetation arrangements for the prevention of debris flow. Therefore, it is worth investigating how specific vegetation arrangements (e.g., stem/row spacing and direction) can regulate debris flows. In particular, whether the interception and retarding effect of vegetation on moving debris flows is related to the type and traits of vegetation or to the arrangement (Isselin-Nondedeu & Bédécarrats, 2007) requires further analysis.

To date, field research has shown that tree trunks and branches can significantly intercept and block debris flows, whereas shrubs can reduce debris flow velocity and reduce the expanse of debris flow movement by increasing the surface roughness in addition to blocking debris flow (Guthrie et al., 2009; Malik et al., 2013; May, 2002). To detect the specific influence of vegetation on sediment interception and trapping, Burylo et al. (2012) made the first attempt to explore and analyze vegetation's ability to trap sediment in laboratory conditions, selecting six traits related to the plant species, leaves, and stem morphology. The results show that the canopy density, leaf size, and plant shape are relevant traits for evaluating and predicting the species' efficiency for sediment trapping. Subsequent studies have shown that other factors appear to affect sediment trapping by vegetation including the type of vegetation (trees, shrubs, and grasses) (Cui et al., 2019b); plant roundness index (Erktan et al., 2013; Richet et al., 2017); length, width, and slope of the vegetation filter strip (Gian et al., 2021; Léa et al., 2018).

The type of vegetation, and its height and density can significantly affect vegetation filter strip performance. The use of plants as a building material transforms the plant's multifunctionality within engineering structures to meet the rising demand for more environmentally friendly approaches to structure design (Gian et al., 2021). In conclusion, to effectively achieve sediment interception while being economical, when designing a vegetation filter strip for debris flow, the layout parameters that affect the density of vegetation, such as the row and stem spacing of plants, should be defined (Ishikawa et al., 2003). The Pudasaini and Fischer (2020)

mechanical model for phase separation offers a solution to physically separating particles from fluid in a debris mixture. However, the effects of vegetation arrangements on the debris flow velocity, flow rate, and particle sorting have rarely been studied, and are often judged based on experience (Dalton et al., 1996).

The objectives of the current study are (1) to investigate the effects of shrubs on debris flow interception, including the effects on flow velocity, flow rate, grain size, and sediment interception: and (2) to identify the shrub layout mechanism that best explains the interception capacity through the comparison of stem and row spacing variations. Sixteen sets of flume experiments, which contained 7 rows with stem spacings of 3, 4, 5, and 6 cm, and row spacings of 4, 6, 8, 10, and 12 cm. The experiments examined the effects of different arrangement parameters on the flow velocity, flow rate, particle size, and sediment interception for dilute and viscous debris flows. Shrubs play a key role in the interception of debris flows and understanding the layout features can be used to optimize vegetation arrangements for practical applications while reducing material inputs to achieve green and economic objectives. It is expected that the current study will provide a theoretical basis for the development of practical measures to prevent debris flows.

2. Materials and methods

2.1. Experimental configuration

The flume experiments were designed to simulate and explore the interception mechanism of a typical debris flow area in a Jiangjiagou Gully (gully slope of $0^{\circ}-13^{\circ}$) (He et al., 2018). Descriptions and functions of the main components of the apparatus are as follows.

- 1) The experiments were done using a flume 4 m long, 0.4 m wide, and 0.4 m deep with a slope of 10° (Fig. 1). Upstream from the flume was a funnel-shaped material pool with a volume of 0.25 m³, which held the reconstructed debris flow sieved to match the bulk density of actual debris flows in the Jiangjiagou Gully (Table 1), which is a typical debris flow area in China (Lin, 2019). The bottom of the inner-funnel-shaped pool had a 30° slope to give the reconstructed debris flows a certain level of momentum and speed (the average velocity of viscous and dilute debris flows are 1.12 and 1.48 m/s, respectively), enabling them to reach the 'debris flow gully' at the bottom. Once the reconstructed debris mixture was released, the material pool acted as the source region for the simulated debris flow. The tailing pool also had a volume of 0.25 m³, and it was used to collect the outflow. In addition, to ensure that the movement of the debris flow was driven by gravity instead of pressure caused by fluid in the tank, a buffer area was set 2.5 m along the flume from the gate of the material pool; this distance is sufficient to eliminate the effect of fluid pressure (Wang et al., 2017a). A measuring ruler was placed along the direction of flowing water on the side of the flume, and a grid was placed on the glass retaining wall to record the height and morphology of sediment deposition in the shrubs (Fig. 1). The actual shrub planting was based on empirical stem spacings of 1.5, 2, 2.5, and 3 m, and row spacings of 2, 3, 4, 5, and 6 m. According to the size of the flume, the vegetation model is scaled according to a 50:1 ratio. The baffles consisted of seven rows, and the corresponding stem spacings of the experimental shrub material were 3, 4, 5, or 6 cm; the row spacings were 4, 6, 8, 10, or 12 cm.
- 2) During the investigation into the effects of stem spacing on the characteristics of debris flow runoff, row spacing was fixed at 12 cm. Similarly, during the investigation into the effects of row

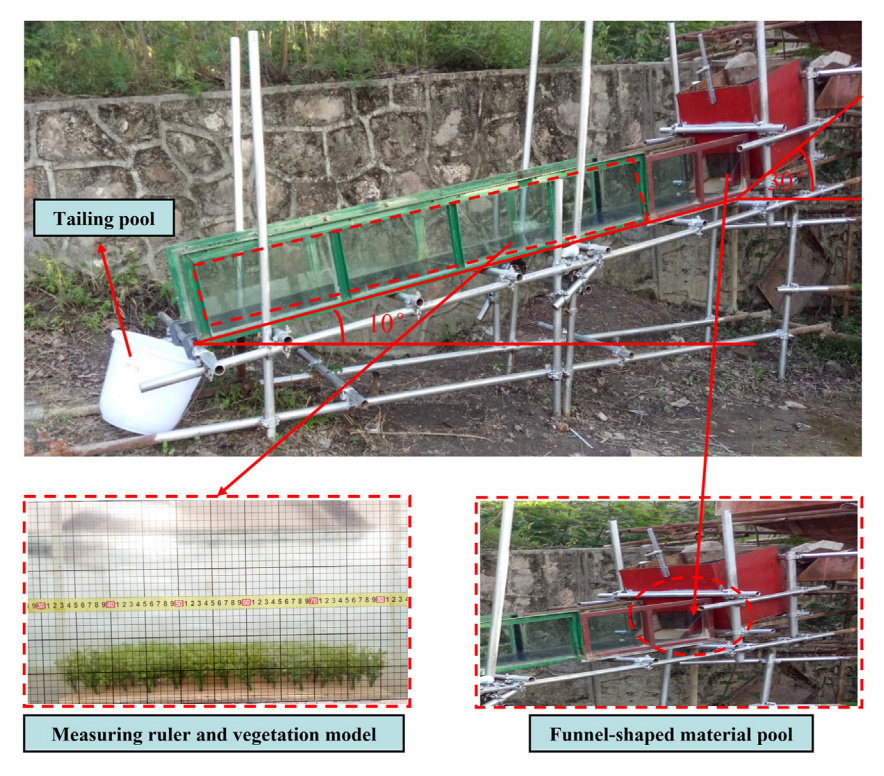


Fig. 1. Layout of the experimental device.

spacing on the characteristics of debris flow runoff, the stem spacing was fixed at 3 cm. Finally, 16 tests were done to study the effects of a shrub filter strip on the runoff characteristics of viscous and dilute debris flows (bulk densities of 2.0 and 1.5 g/cm³, respectively). The parameters for the tests are listed in Table 1. Although, small-scale flume tests often are constrained by the principles of geometric similarity, material similarity, and dynamic similarity (Choi et al., 2014; Ng et al., 2015; Zhou et al., 2019), the current study focused on the regulation and mechanism of debris flow by the shrub filter strip flume, which is not an equivalent scaling test study of a specific debris flow event, so material similarity (solid-phase material from the real Jiangjiagou debris flow in the field) was taken as the starting point, the dynamic similarity condition of debris flow then was considered, and the flume model was designed according to the gravity similarity criterion. Geometric similarity is achieved by controlling the length scale, $\lambda_1 = 50$. Moreover, dynamically similar conditions often depend on the dimensionless Froude number, Fr, which characterizes the ratio of inertial force to the gravity for a flowing material. The Fr for small-scale flume tests is required to be consistent with that of natural debris flows. The Froude number is expressed by $Fr = \frac{v}{\sqrt{gh \cos \theta'}}$ where v represents the velocity before the baffles (m/s), g is the gravitational acceleration (m/s^2) , h is the flow depth (m), and θ is the channel slope $(^{\circ})$. According to the literature (Heller, 2011; Lobovský et al., 2014), the Fr of natural debris flows are mostly less than 5.0. In the experiments, the Fr values of incoming debris flows in the flume (Fig. 2) are basically in the range of 2.5 < Fr < 3.2, which are within the Fr range of field debris flow events (Hübl et al., 2009; Kwan et al., 2015; Mcardell et al., 2007), implying that the conditions of the experimental study can be considered as representative of natural debris flows. It is worth pointing out that under natural conditions in the transverse direction, the flow depth, riverbed,

and velocity are different at the sidewalls and in the center.

However, in the current study, more attention is paid to the full interception benefit, therefore, although it is different from natural conditions, and the current study focuses on the average level.

2.2. Instrumentation

Two digital cameras (Canon LEGRIA; denoted as cameras #1 and #2) with a resolution of 1,440 \times 1,080 pixels and frame rate of 50 frames per second (fps) were used to measure the velocities of the debris flows before and after the shrub filter strips, respectively. In addition, two laser sensors (Leuze, ODSI; denoted as lasers #I and #II) with a resolution of 1 mm were installed at the same positions as cameras #1 and #2. These devices were used to measure the evolving flow depths before and after the shrub filter strips, respectively. The third camera (denoted as camera #3) was positioned on one side of the flume to record the entire debris flow process. The fourth camera (denoted as camera #4) was installed in front of the flume channel to record the time taken for the debris flows to move from the top to the bottom of the flume as shown in Fig. 2.

2.3. Experimental materials

The reconstructed debris flow materials consisted of debris flow deposits from the Jiangjiagou Gully that passed through a 2 cm sieve (Fig. 3), and then were mixed with water to form viscous and dilute debris flows with bulk densities of 2.0 and 1.5 g/cm³, respectively. The shrub models were made from plastic with six branches with a height of 5 cm and a stem diameter of 0.3 cm (Fig. 4). Each shrub model was fixed into holes in a plank. The current study focused on the mechanical properties and morphological parameters, in which one of the most important mechanical properties for structural analysis of bending is the modulus of elasticity (Al-Zube et al., 2018). The elastic modulus of the *Coriaria sinica* simulated in this paper is

Table 1Parameters for the shrub filter strip tests.

Test No.	1	2	3	4	5	6	7	8
Stem spacing (cm)	3	3	4	4	5	5	6	6
Row spacing (cm)	12	12	12	12	12	12	12	12
Row number	7	7	7	7	7	7	7	7
Bulk density (t/m ³)	1.5	2.0	1.5	2.0	1.5	2.0	1.5	2.0
Length of shrub filter strip (m)	0.72	0.72	0.72	0.72	0.72	0.72	0.72	0.72
Test No.	9	10	11	12	13	14	15	16
Test No. Stem spacing (cm)	9	10 3	11 3	12 3	13	14 3	15 3	16
Stem spacing (cm)	3	3	3	3	3	3	3	3
Stem spacing (cm) Row spacing (cm)	3 4	3 4	3 6	3	3 8	3 8	3 10	3 10

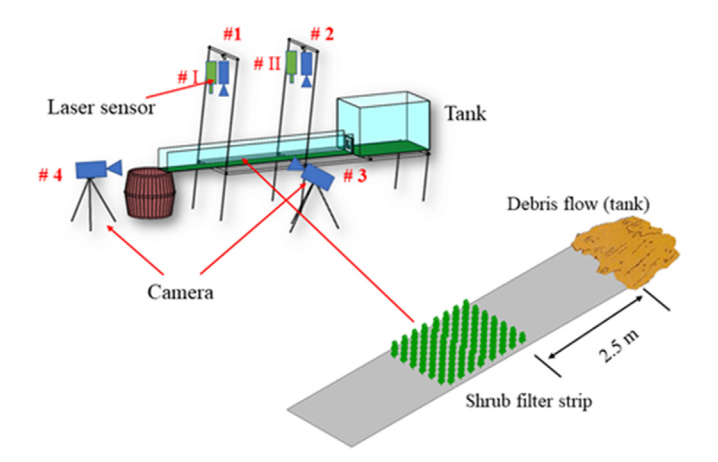


Fig. 2. Layout of a shrub filter strip during an experimental simulation test. The components of the experiment include material pool (tank), flume, tail pool, shrub filter strip, debris flow material, and measuring apparatus (laser sensors and cameras).

between 10 and 20 GPa, and alternative plastics within this elastic modulus were selected.

2.4. Data acquisition and processing

Before starting the experiment, all cameras were turned on; then, the configured debris flow was poured into the tank and stirred slightly, and the gate was quickly opened to the set height (i.e., gate opening of 4 cm) so that the test debris flow would flow out. The gate opening height was the same for each test. When the debris flow in the flume stopped flowing, the cameras were turned off, and the samples were collected (Fig. 5).

Data were collected and used to calculate three properties of the debris flow.

- 1) Bulk density in the tail pool. Viscous debris flow refers to a debris flow containing a large amount of clay soil, and solid material accounting for 40%-60%, even up to 80%, yielding a bulk density >1.8 g/cm³. Dilute debris flow refers to a debris flow which water is the main component, and clay soil content is small. Solid material accounts for 10%-40% with great dispersion, presenting a bulk density of 1.5–1.8 g/cm³. For more descriptions on the dense and dilute debris flows, as well as viscous debris flows, their mechanical properties, and dynamical consequences, refer to Pudasaini & Krautblatter (2019). In the current study, the particle size distribution of original materials was available, therefore, the density was simply used to classify viscous or dilute debris flows. After each experiment, the debris in the tail pool was collected, and the weight (*m*) and volume (v) were measured. This was used to calculate the bulk density, ρ , according to the equation: $\rho = \frac{m}{V}$.
- 2) Flow depth. The flow depth *h* was measured using the laser sensors.
- 3) Velocity. Cameras #1 and #2 were positioned above the baffles to obtain the surface velocity of the debris flow before and after the shrub filter strip. This measurement was achieved by recording the distance s (m) traveled by a reference material (e.g., a table tennis ball) in a given time t (s). Thus, the velocity v (m/s) can be calculated using the equation: $v = \frac{s}{r}$.

3. Results

3.1. Bulk density reduction

Table 2 shows the effects of the shrub filter strip on the bulk densities of the dilute and viscous debris flows. As the stem spacing and row spacing changed, the bulk density reduction for viscous debris flow varied between 0.5% and 3.5%, and 0.5% and 5.3%, respectively.

For the dilute debris flow, as the stem spacing increased, the bulk density of the debris outflow gradually increased, and the bulk density reduction gradually decreased (Table 2). The bulk density reduction was 8% when the stem spacing was the largest (6 cm),

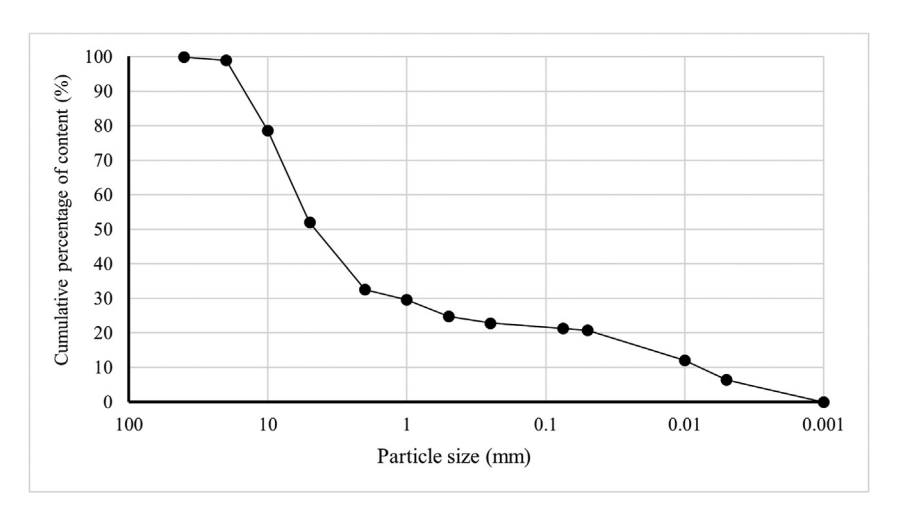


Fig. 3. Particle size distribution of original materials from the Jiangjiagou Gully.



Fig. 4. Shrub model.

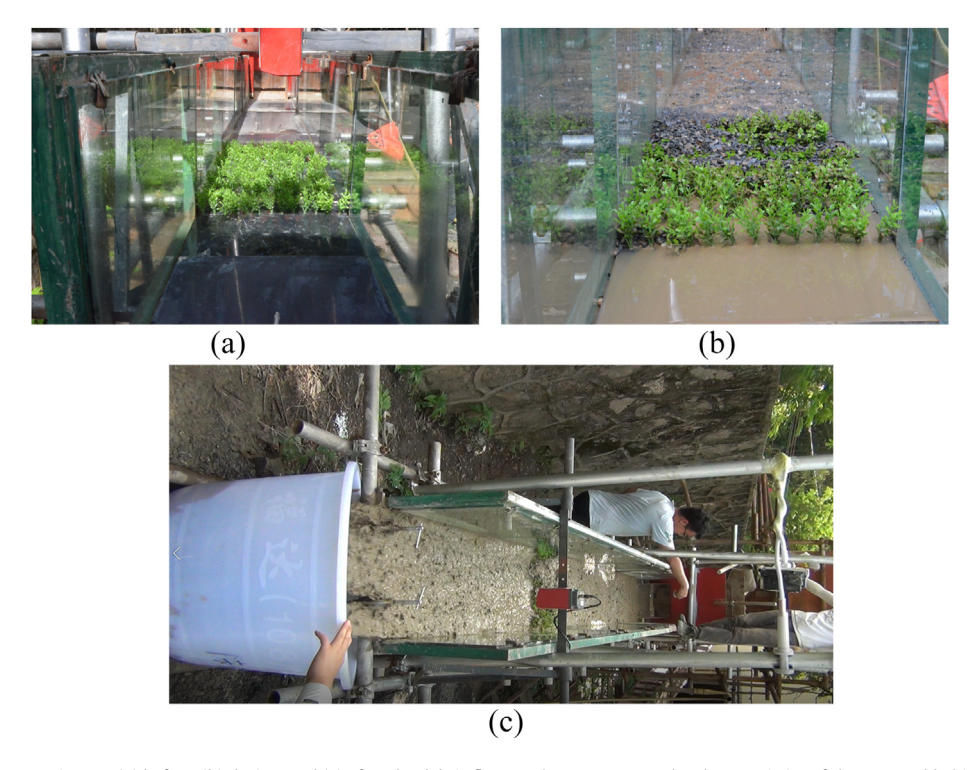


Fig. 5. Process of the flume experiments (a) before, (b) during, and (c) after the debris flow. In these processes, the characteristics of the pre- and behind-shrub filter of the debris flow were recorded, the outflow material was weighed, and the volume and particle fraction were analyzed.

and it was increased to 17.9% when the stem spacing was the smallest (3 cm). Thus, the shrub filter strip produced a relatively good bulk density reduction effect on the dilute debris flow when the stem spacing was small. As the row spacing increased, the bulk

density of the debris outflow first decreased and then increased, and the bulk density reduction first increased and then decreased. The greatest bulk density reduction rate (27.6%) was achieved at a row spacing of 8 cm. A comprehensive comparison shows that the

Table 2Bulk density reduction with different stem and row spacings.

Stem spacing (cm)	Bulk density reduction (%)		Row spacing	Bulk density reduction (%)		
	Dilute debris flow $(\rho = 1.5 \text{ g/cm}^3)$	Viscous debris flow $(\rho = 2.0 \text{ g/cm}^3)$	(cm)	Dilute debris flow $(\rho = 1.5 \text{ g/cm}^3)$	Viscous debris flow ($\rho = 2.0 \text{ g/cm}^3$)	
3	17.9	0.5	4	20.7	2.1	
4	16.4	0.5	6	22.5	1.5	
5	14.5	3.5	8	27.6	1.5	
6	8.0	0.7	10	19.2	5.3	
			12	17.9	0.5	

Please cite this article as: He, S et al., Experimental investigation of the effects of shrub filter strips on debris flow trapping and interception, International Journal of Sediment Research, https://doi.org/10.1016/j.ijsrc.2022.09.005

shrub filter strip produced a better bulk density reduction effect when the debris flow was dilute and had a negligible impact on the viscous debris flow.

3.2. Flow rate regulation

Figures 6 and 7 show the changes in the volumetric flow rates with different stem and row spacings, when the debris flow passed through the shrub filter strip. As the stem spacing increased, the peak flow of both the dilute and viscous debris flows gradually increased once they passed through the filter strip, and the flow reduction rates gradually decreased (Fig. 6). Thus, when the stem spacing was smallest (3 cm), the flow reduction effect was the greatest for both the dilute and viscous debris flows. The flow reduction for the dilute and viscous debris flows were 26.3% and 42.7%, respectively. As the row spacing increased, the peak flow rate of the dilute debris flow gradually increased once it passed through the filter strip, and the flow reduction gradually decreased. In contrast, the peak flow rate of the viscous debris flows first decreased, then increased, and the flow reduction first increased and then decreased. The flow reduction for the viscous debris flow was greatest, reaching 47.4%, when the row spacing was 10 cm (Fig. 7).

3.3. Characteristics of the flow velocity

Figures 8 and 9 show the changes in the debris flow velocity caused by changes in the stem and row spacings, respectively. As the stem spacing increased (Fig. 8), the flow velocities of both the dilute and viscous debris flows increased after they passed through the filter strip, and the flow velocity reduction gradually decreased. Thus, when the stem spacing was smallest (3 cm), the flow velocity reduction was greatest (25.5% and 29.5% for dilute and viscous debris flows, respectively). In addition, when the stem spacing was largest (6 cm), the flow velocity reduction was smallest (18% and 15.7% for dilute and viscous debris flows, respectively). As the row spacing increased (Fig. 9), the flow velocity of the dilute debris flow also gradually increased after the filter strip, and the flow velocity reduction gradually decreased. Thus, when the row spacing was smallest (4 cm), the flow velocity reduction was greatest (44.9%). However, the flow velocity of the viscous debris flows first decreased, then increased after the filter strip, and the flow velocity reduction first increased, then decreased. Thus, the flow velocity reduction was greatest (34.3%) when the row spacing was 10 cm.

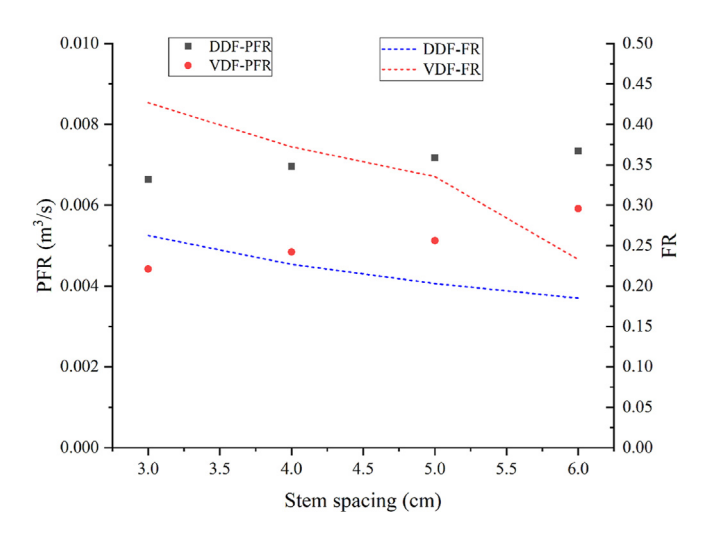


Fig. 6. Peak flow rate (PFR) and flow reduction (FR) for different stem spacings. DDF, dilute debris flow; and VDF, viscous debris flow.

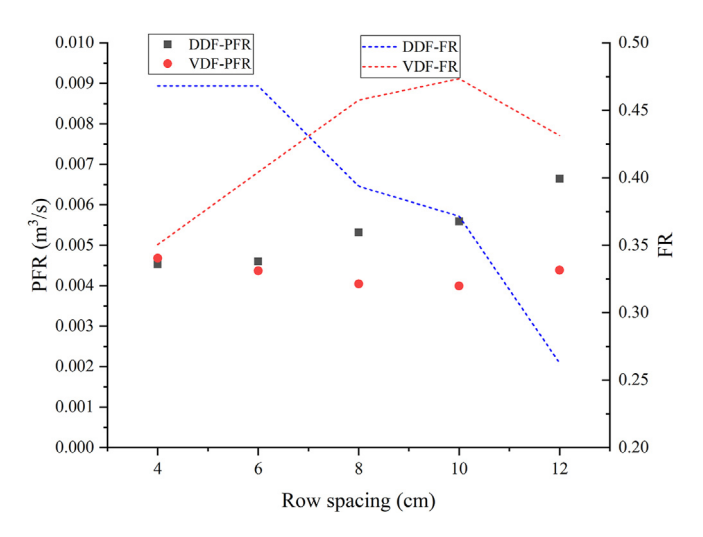


Fig. 7. Peak flow rate (PFR) and flow reduction (FR) for different row spacings.

3.4. Sediment interception

As shown in Fig. 10, the amount and fraction of sediment interception decreased gradually as the stem spacing increased for both dilute and viscous debris flows. Thus, when the stem spacing was smallest (3 cm), the sediment interception rates were greatest (60.9% and 60% for dilute and viscous debris flows, respectively). In addition, when the stem spacing was largest (6 cm), the sediment interception was lowest (27.4% and 39% for dilute and viscous debris flows, respectively). As shown in Fig. 11, the amount and fraction of sediment interception first increased, and then decreased, as the row spacing increased for both dilute and viscous debris flows. The sediment interception was greatest at a row spacing of 6 cm (70.7%) for the dilute debris flow, and 10 cm (66.3%) for the viscous debris flow.

3.5. Relations between velocity and outflow volume reduction

Table 3 lists the flow velocity reduction and sediment interception fraction for dilute and viscous debris flows with different stem and row spacings. The fitting characteristics between the two values are shown in Fig. 12. The interception of the dilute debris flow exhibited a parabolic relation, where the sediment

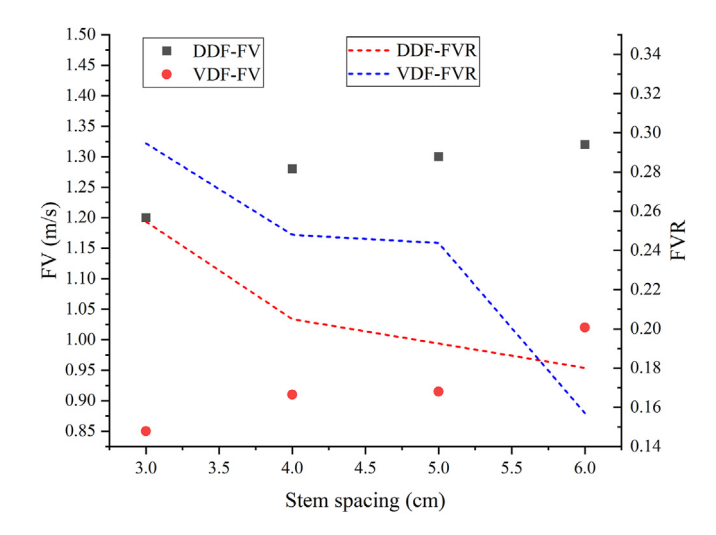


Fig. 8. Flow velocity (FV) and flow velocity reduction (FVR) for different stem spacings after the debris flow passed through the filter strip.

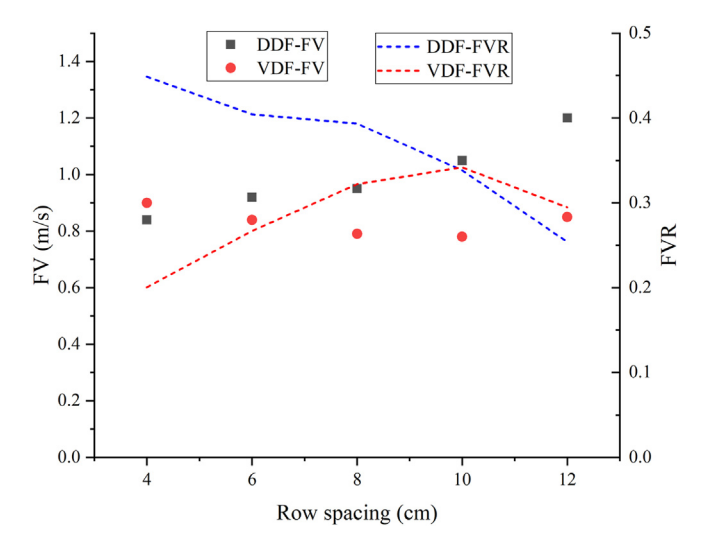


Fig. 9. Flow velocity (FV) and flow velocity reduction (FVR) for different row spacings after the debris flow passed through the filter strip.

interception fraction first increased and then decreased, as the flow velocity reduction increased. This trend occurs because of the water—stone separation effect. Initially, there are more large particles in the dilute debris flow, and the interception effect is obvious. The material flow velocity and flow reduction exhibit a corresponding relations. As the flow path lengthens, large particles are gradually intercepted and deposited, so the flow velocity reduction at this point is primarily reflected by the mud and water flow velocity, and there are relatively few large particles. Therefore, the flow velocity reduction continues to increase, but the interception of large particles decreases, so the sediment interception fraction drops. For viscous debris flows, there is no water—stone separation, so the reduction in the material flow velocity can be approximated as corresponding to the interception of sediment. Therefore, the two factors exhibited a linear relation.

4. Discussion

4.1. Differences between dilute and viscous debris flows

The experimental results show that changes in the stem and row spacings of the shrub filter strip can have a significant effect on the interception efficiency for both dilute and viscous debris flows.

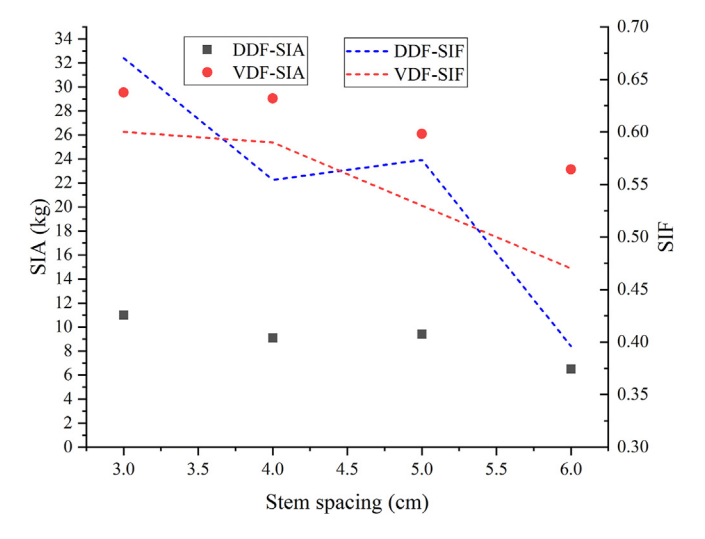


Fig. 10. Sediment interception amount (SIA) and sediment interception fraction (SIF) for different stem spacings.

Figure 13 shows the movement of dilute debris flows with different row spacings (the same stem spacing) conditions. The overall interception effect was significant. In particular, most of the coarse particles remained above and inside the filter strip, representing a significant separation of water and stone (coarse particles). Over time, the slurry continued to slow along the slope. Clearly, the interception reduced the motion and velocity of the dilute debris flows. Moreover, the separation effect was more significant when the spacing was greater. These data can be utilized to validate the mechanical phase separation model for debris mixtures consisting of solid particles and viscous fluid by Pudasaini and Fischer (2020) describing how solid particles and fluid can be separated during a debris flow.

In contrast, the water—coarse particle separation was not observed for the viscous debris flows shown in Fig. 14. Instead, the shrub filter strip was gradually covered by the debris flow and wave-like depositions were observed.

In the unsubmerged state, the density reduction of the out-flowing dilute debris flow is because the plant spacing has a good water-stone separation effect, and the coarse particles are intercepted in the vegetation zone. While the viscous debris flow always performed the overall sediment movement, its density is reduced for two reasons: on the one hand, when the viscous debris flow gradually stops and deposits in the vegetation zone, the fluid flows out by seepage; on the other hand, the vegetation intercepts most of the viscous debris flows. A small amount of the viscous mixture flows out, and the density of this part does not change much, but it is diluted by the subsequent flowing water, resulting in density reduction.

As indicated by the experimental observations and a comparison of the particle size distribution before/after the filter strip, changes in the stem spacing had a greater effect on the average particle size of the outflowing sediment than changes in the row spacing. However, there were also differences between the dilute and viscous debris flows. For the dilute debris flow (Fig. 15a), as the stem spacing increased, the proportion of coarse particles in the sediment increased and the proportion of fine particles decreased. This was caused by the significant separation of water and stone, and the weak mutual adhesion between particles, which amplified the changes in the filtering effect caused by the stem spacing. However, as the row spacing increased (Fig. 15b), there was no evident change in the average particle size of the outflowing sediment. Comprehensive analysis showed that, for dilute debris

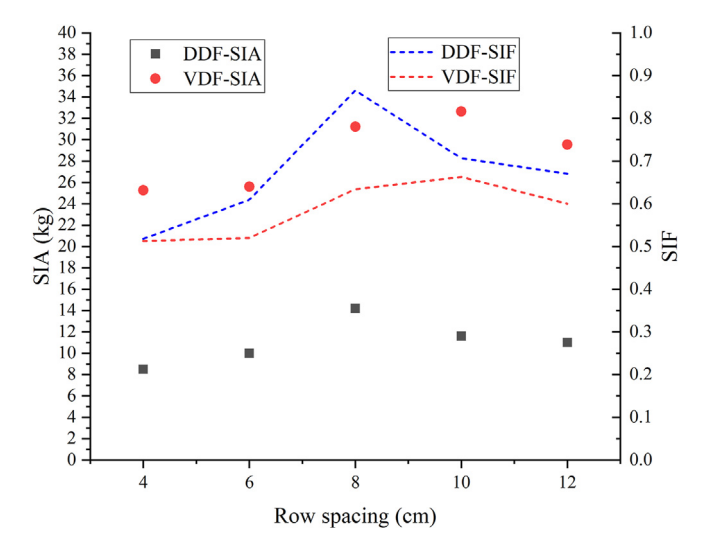


Fig. 11. Sediment interception amount (SIA) and sediment interception fraction (SIF) for different row spacings.

Table 3Flow velocity reduction (FVR) and sediment interception fraction (SIF) of shrub filter strip.

Stem spacing D_x (m)	Row spacing D_y (m)	Viscous $(\rho = 2.0 \text{ g/cm}^3)$		Dilute $(\rho = 1.5 \text{ g/cm}^3)$		
		FVR	SIF	FVR	SIF	
0.03	0.04	0.201	0.513	0.449	0.615	
0.03	0.06	0.267	0.52	0.404	0.707	
0.03	0.08	0.322	0.634	0.373	0.687	
0.03	0.1	0.342	0.663	0.308	0.652	
0.03	0.12	0.295	0.6	0.254	0.609	
0.04	0.12	0.248	0.57	0.205	0.53	
0.05	0.12	0.244	0.5	0.193	0.415	
0.06	0.12	0.157	0.39	0.18	0.274	

flows, the stem spacing regulated the interception of coarse particles and the passing of fine particles by the shrub filter strip.

In contrast, viscous flows were relatively adhesive, and they moved as a whole, so the shrubs had an overall interception effect, and there was no water—stone separation. Therefore, changes in the stem or row spacing have a negligible effect on the particle size distribution of the sediment outflow for the viscous debris flows (Fig. 16). In this case, a large-scale debris flow would submerge the shrub filter strip. However, the strip would increase the surface roughness and friction of the slope, thereby reducing the kinetic energy of the debris flow. In contrast, small-scale debris flows would not submerge the filter strip, and the strong adhesion of the flow ensures that overall interception occurs, and the flow remains above or within the filter strip. Over time, the debris flow slurry would gradually seep out, and there would be an obvious outflow of "water—sediment."

Although stem spacing had a dominant effect on debris flow interception, the effect of row spacing should not be ignored. For dilute debris flows, the flow velocity and flow rate reduction both decreased gradually as the row spacing increased. That is, when the row spacing was smaller, the shrub filter strip produced a greater reduction in the debris flow velocity and flow rate, and the interception effect was greater. This is because decreasing the row spacing increases the shrub coverage density in the flow direction, which increases the barrier gradient, reduces the kinetic energy of the flow, and produces the interception effect. For viscous debris flows, the flow velocity and flow rate reduction first increased and then

decreased as the row spacing increased. That is, when the row spacing was smaller, the flow velocity and flow reduction were smaller. This is because viscous debris flows move as a whole, and they exhibit strong adhesion with insignificant water—stone separation. Furthermore, the shrubs are submerged in most cases, so small row spacings will not have a noticeable drag reduction effect on viscous debris flows over a brief period. However, as the row spacing increases, the buffering effect of the shrub filter strip is amplified, and reductions in the flow velocity and flow rate become more significant.

From the foregoing analysis, the density of the shrub filter strip can be controlled by adjusting stem and row spacings. Regardless of whether the debris flow is dilute or viscous, the optimal interception effect is not determined by a single factor—either the stem or row spacing—but by a combination of the two. In terms of the amount of sediment intercepted, for dilute debris flows, sediment interception rates of 70.7% can be achieved using stem and row spacings of 3 and 6 cm, respectively (corresponding to actual spacings of 1.5 and 3 m, respectively). For viscous debris flows, sediment interception rates of 66.3% can be achieved using stem and row spacings of 3 and 10 cm, respectively.

4.2. Effect of arrangement parameters on flow velocity

Shrubs are not generally submerged when they intercept dilute debris flows, but they are submerged by viscous debris flows. Gu et al. (2007) reported that, when they are not submerged, the roughness of flexible plants decreases gradually as the water depth increases; however, when they are submerged, the roughness increases gradually if the water depth is low. Therefore, changes in the submerged state may affect the roughness coefficient; however, this is a complex process when the debris flow is viscous and is outside the scope of this paper. The following is a discussion about the relations between the arrangement parameters and flow velocity of dilute debris flows.

As shown in Fig. 17, a filter strip with stem spacing, D_x , row spacing, D_y , and N rows will have length $L = (N-1) \times D_y$. If the channel width is B, then, owing to the staggered planting of the filter strips, the number of shrubs will be [B/D] (rounded) or $[B/D_x] + 1$. Let the channel slope be θ . By using the 0-0 horizontal plane as the reference plane, sections upstream (a-a) and downstream (b-b) from the shrub filter strip can be selected. Upstream from the shrub filter strip the flow velocity is V_a , the elevation is Z_a ,

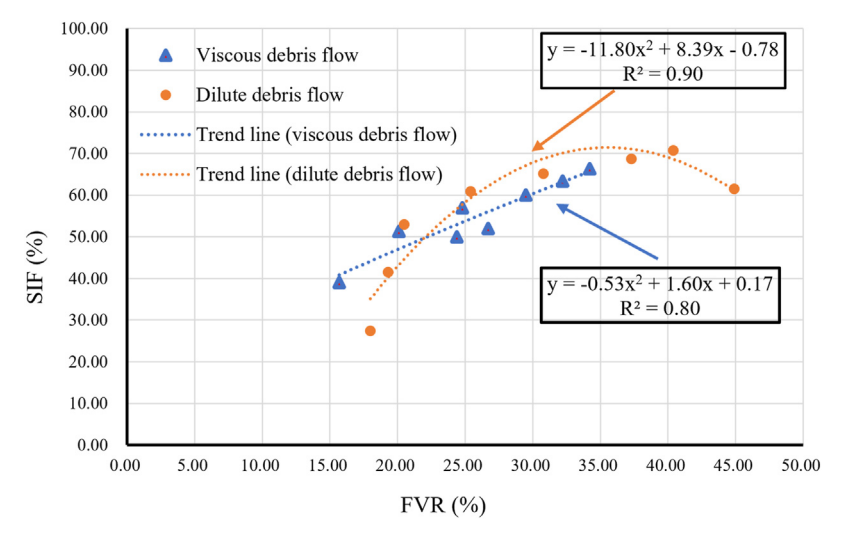


Fig. 12. Flow velocity reduction (FVR) fitted to the sediment interception fraction (SIF).

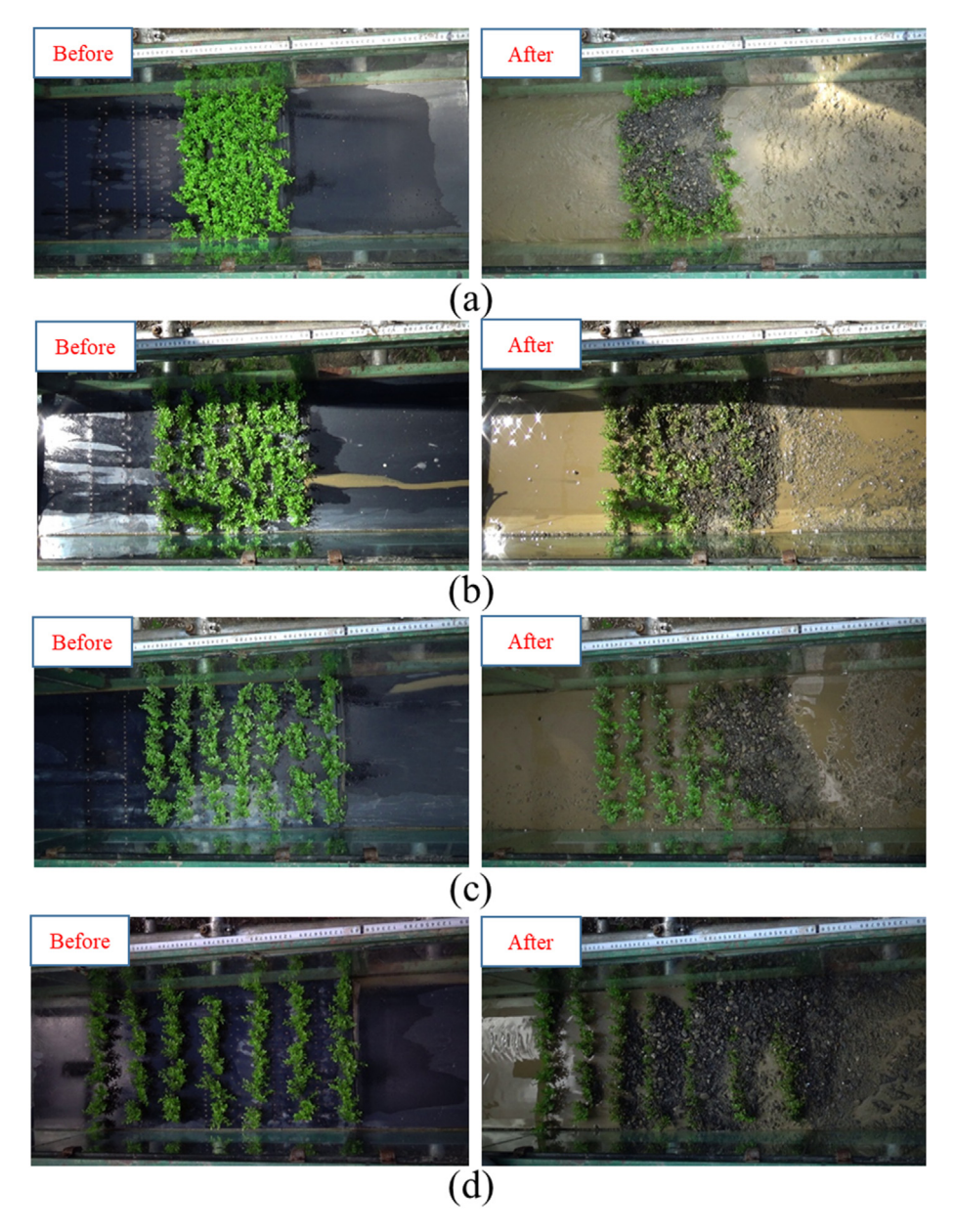


Fig. 13. Interception of dilute debris flows by different shrub filter strip arrangements with row spacings of (a) 4, (b) 6, (c) 8, and (d) 10 cm and stem spacing of 3 cm.

the flow depth is h_a , the specific weight is γ_a , and the pressure is p_a . Similarly, downstream from the shrub filter strip the flow velocity is V_b , the elevation is z_b , the flow depth is h_b , the specific weight is γ_b , and the pressure is p_b .

In dilute debris flows, shrubs mainly intercept gravel (coarse particles), so the outflow consists of slurry and small particles. Therefore, if the slurry before and after the filter strip is a constant fluid (the components of the particles and viscosity were not changed), then the flow parameters (specific weight, pressure, density, etc.) will be invariant with time. Without considering the vertical and horizontal distributions of the flow velocity, $h_{\rm f}$ may be used to represent the frictional head loss or frictional energy loss of the debris flow. According to the law of conservation of mechanical energy of a fluid, the Bernoulli equation must be satisfied as the sum of kinetic energy, gravitational potential energy, and pressure potential energy is a constant. This can be expressed by

$$z_{\rm a} + \frac{p_{\rm a}}{\rho g} + \frac{v_{\rm a}^2}{2g} = z_{\rm b} + \frac{p_{\rm b}}{\rho g} + \frac{v_{\rm b}^2}{2g} + h_{\rm f} \tag{1}$$

and

$$\Delta z + h_a \cos \theta + \frac{p_a}{\gamma_a} + \frac{v_a^2}{2g} = h_b \cos \theta + \frac{p_b}{\gamma_b} + \frac{v_b^2}{2g} + h_f$$
 (2)

where $\Delta z = z_a - z_b$. Equation (2) can be simplified to $h_f = \Delta z + (h_a - h_b) \quad \cos\theta + \frac{p_a \gamma_b - p_b \gamma_a}{\gamma_a \gamma_b} + \frac{v_a^2 - v_b^2}{2g}$ (3)

and

$$\Delta z = L \times \sin\theta = (N-1) \times D_{y} \times \sin\theta \tag{4}$$

The frictional head loss or frictional energy loss, $h_{\rm f}$ can be calculated using the Darcy–Weisbach formula:

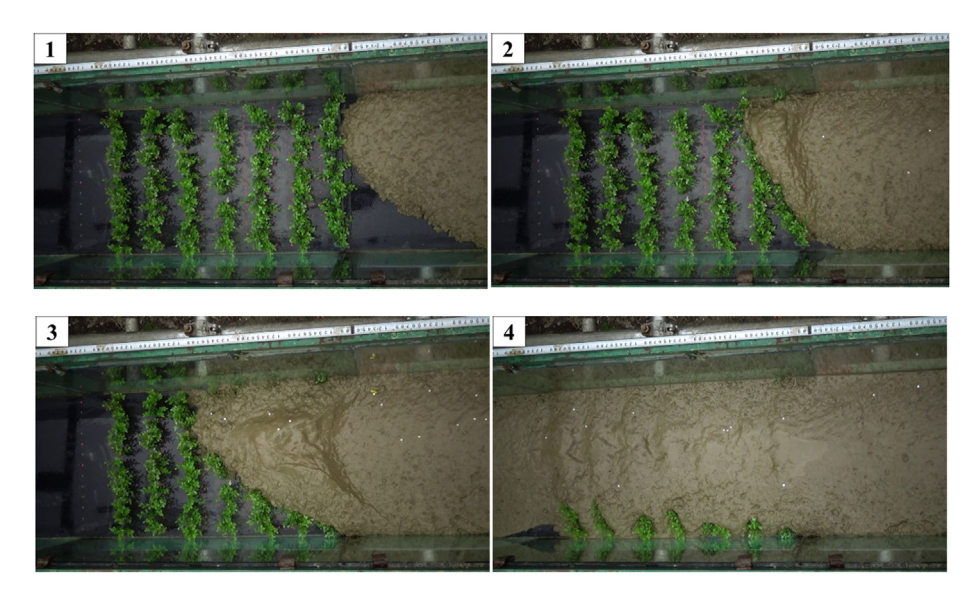
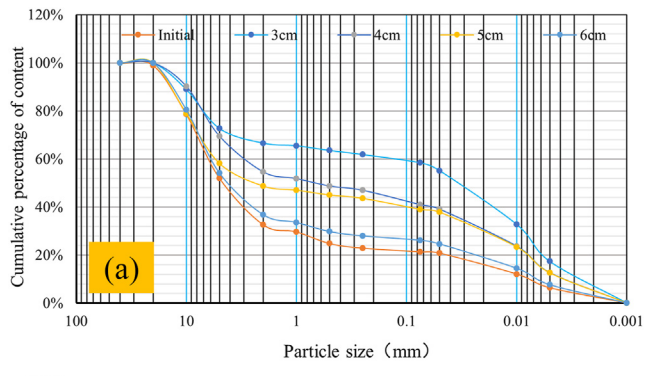


Fig. 14. Interception phenomenon of a viscous debris flow by a shrub filter strip.

$$h_{\rm f} = \lambda \frac{L}{d} \frac{V^2}{2g} \tag{5}$$

where λ is the friction coefficient along the flow path, L is the length of the shrub filter strip, and V is the average flow velocity of the section. The Darcy—Weisbach formula essentially calculates the frictional head loss in a circular pipe, so d in Eq. (5) represents the pipe diameter. To make this formula applicable to an actual debris flow gully or flume model test, the diameter of a circular pipe with the same hydraulic radius is used as the equivalent diameter $d_{\rm e}$ of the non-circular section, according to known fluid principles. The circular section is given as



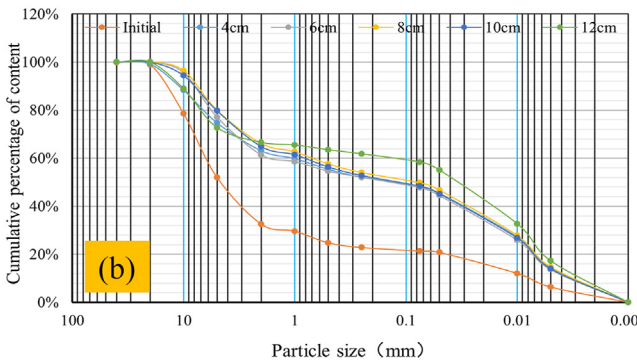


Fig. 15. Effect of the shrub filter strips on the particle size distribution (PSD) in a dilute debris flow. (a) PSD affected by stem spacing and (b) PSD affected by row spacing.

$$d = 4R_{\text{circle}} \tag{6}$$

where $R_{\rm circle}$ is the hydraulic radius of a circular section, and the non-circular section is

$$4R_{\text{circle}} = 4R = d_{\text{e}} \tag{7}$$

where R is the hydraulic radius of the debris flow channel. The equivalent diameter is four times the hydraulic radius, and for a rectangular section with length, a, and width, b, the equivalent diameter is

$$d_{e} = 4R = 4 \times \frac{ab}{2(a+b)} = \frac{2ab}{a+b}$$
 (8)

Combining the flume model a in Eq. (8) is equivalent to the gully or flume width B, and b is equivalent to the flow depth, h, in the gully or flume. Thus,

$$h = \frac{Q}{VB} \tag{9}$$

where Q is the volumetric flow rate. Substituting Eq. (9) into Eq. (8) yields

$$d_{\rm e} = \frac{2QB}{VB^2 + Q} \tag{10}$$

Then, replacing d in Eq. (5) with d_e yields

$$h_{\rm f} = \frac{\lambda V^2 L \times \left(V B^2 + Q \right)}{40 B g} \tag{11}$$

The friction coefficient along the flow path λ can be derived from the Chezy formula or the Manning formula. That is,

$$V = \sqrt{\frac{8g}{\lambda}} \sqrt{RJ} = C\sqrt{RJ}$$
 (12)

$$C = \frac{1}{n} R^{1/6} \tag{13}$$

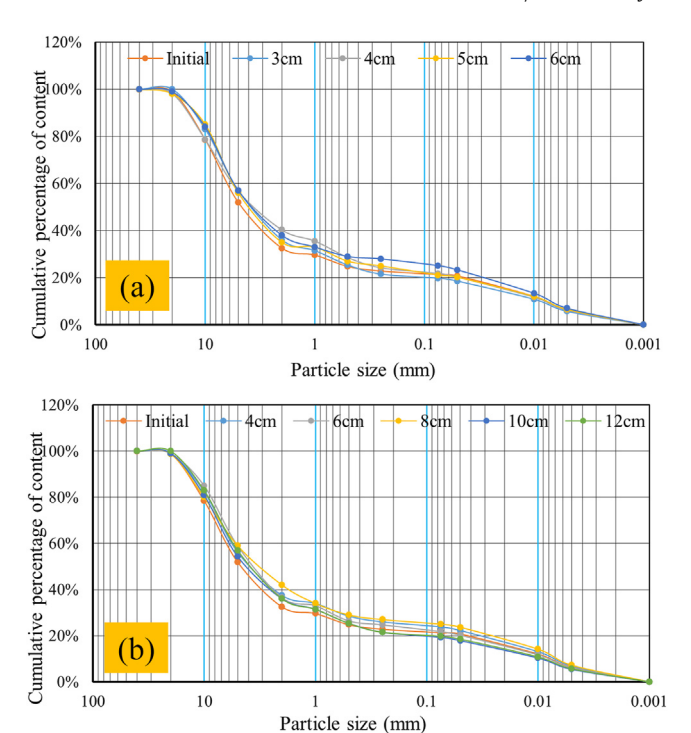


Fig. 16. Effect of the shrub filter strips on the particle size distributions (PSD) in a viscous debris flow. (a) PSD affected by stem spacing and (b) PSD affected by row spacing.

$$\lambda = \frac{8n^2g}{p_{\uparrow}^4} \tag{14}$$

and

$$R = \frac{A}{\chi} = \frac{(B - md)h_{s}}{2h_{s}(m+1) + B - md}$$
 (15)

where J is the hydraulic gradient, C is the Chezy roughness coefficient, n is the Manning roughness coefficient, m is the number of shrubs per row, d is the shrub trunk diameter, and h_s is the submerged depth of the shrubs. Subsequently,

$$v_{b} = \sqrt{v_{a}^{2} + 2g \left[L \sin \theta - \frac{\lambda VL \times \left(VB^{2} + Q \right)}{4QBg} \right]}$$
 (16)

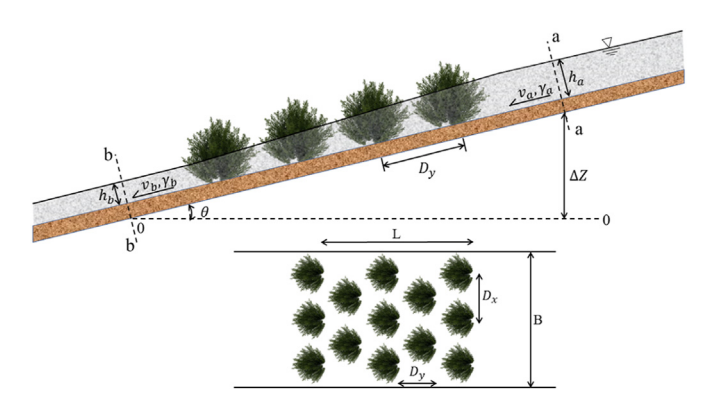


Fig. 17. Schematic representation of the movement characteristics of a dilute debris flow in a shrub filter strip blockage.

From the formula deduced for the flow velocity after the strip (i.e., Eq. (16)), the length of the vegetation strip, L, friction coefficient along the flow path, λ , volumetric flow rate, Q, and channel width B are related. Moreover, the roughness coefficient in the equation for the friction coefficient along the flow path is related to the vegetation arrangement (such as the planting density, which is determined by the stem and row spacings) and the submerged vegetation volume (which is closely related to the shrub height, canopy diameter, etc.). Therefore, arrangements with different stem and row spacings can affect the movement of dilute debris flows.

A relation between the arrangement parameters and changes in the flow velocity was not derived for viscous debris flows. However, analysis of the experimental data (Figs. 8 and 9) shows that changes in the stem and row spacing affect the flow velocity to different extents. This indicates that the flow velocity of viscous debris flows after the vegetation filter strip is closely related to the vegetation arrangement and submerged volume ratio. This should be investigated further and verified in future research.

4.3. Comparisons between the current study and others in the literature

The blocking effect of vegetation on runoff and sediment movement has been described in previous studies. There are many vegetation-related factors including vegetation cover/density, vegetation type and distribution; and plant stem density, diameter, and arrangement that can affect flow regimes, flow hydraulic dynamics, and soil erosion (Hong et al., 2016; Järvelä, 2002; Mu et al., 2019). Mu et al. (2019) show that the sediment transport capacity decreases as the stem basal cover/density increases, and the rate of decrease is considerably higher than other values reported in the literature. Therefore, the current study focused on exploring the effects of stem and row spacings on the movement characteristics of debris flows, which is of great significance. A comparison of the effects of vegetation arrangements on water and debris flow movements shows that both can be affected by changes in the stem and row spacings. However, the row spacing has a relatively small effect on the debris flow, but a relatively large effect on the water flow (Abu-Zreig et al., 2004; Zhang et al., 2018). The main reason for this could be that the stem spacing directly affects the contact between the debris flow fluid and the front of the vegetation, thereby achieving effective deceleration and interception. In addition, the stem spacing reflects the width of the fluid movement channel. Both dilute and viscous debris flows are solid-liquid twophase fluids, and they are much more viscous than water. Furthermore, the presence of solid particles means the blocking effect caused by changes in the stem spaces is more obvious than it is for water.

It should also be considered that the relative soil loss caused by general water erosion is related to the vegetation coverage (Vegetation coverage degree is usually defined as the percentage of the vertical projection area of vegetation (including leaves, stems, and branches) on the ground in the total statistical area, which is an important parameter to describe the vegetation coverage). That is, relative soil loss, SLr, is an exponential function of vegetation cover, C_{v_r} (Durán & Rodríguez Pleguezuelo, 2008; Gyssels et al., 2005). This can be expressed as

$$SLr = e^{-b}q^{c}v \tag{17}$$

where b_q is a constant. In fact, the vegetation coverage is closely related to row and stem spacing (Fu et al., 2020). Therefore, the vegetation coverage in the final analysis is affected by the row and stem spacings. By calculating the relation between the sediment

interception amount and the vegetation coverage under different row and stem spacings, as shown in Fig. 18 (where the debris flow outflow volume corresponds to the soil loss caused by general water erosion), it can be shown that a polynomial relation is observed between the debris outflow volume and vegetation coverage rather than an exponential relation. According to Fig. 18. the relationship can be represented with a quadratic polynomial as $SLr = uC_v^2 + tC_v + k$. Thus, the interception of debris flows by shrubs is more complicated than that of water. The rule regulating shrub arrangements for water cannot be equated to those for debris flows. In principle, the greater the vegetation coverage, the greater the debris interception. However, regardless of whether the debris flow is dilute or viscous, when the flow is large enough to submerge the shrubs, further increases in coverage no longer affect the debris flow movement. Thus, the outflow volume increases as the shrub coverage increases.

4.4. Limitations and future work

Ecological engineering has an increasingly prominent role in disaster prevention (He et al., 2017; Rey et al., 2019). So far, it has been shown that vegetation can suppress debris flow disasters and landslides and regulate the effects of rainfall redistribution, surface runoff, soil erosion, and sediment transportation (Gonzalez-Ollauri & Mickovski, 2017; Reichenbach et al., 2014). The current study only considered the interception effect of shrubs on debris flows in terms of the stem and row spacings. Although the current study reflected the effects of changes in these spacings on interception, there are many other vegetation-related factors that affect water flow patterns, flow hydraulic dynamics, and soil erosion such as cover/density; type and distribution of vegetation; and plant stem density, diameter, and arrangement (Järvelä, 2002; Mu et al., 2019). What's more, the current study uses Bernoulli and Darcy-type equations to model debris flow interception and the associated energy state, and finally derives an equation for velocity after the shrub strip, including several parameters. This equation can simplify the situation to develop some simple model equations, which to some extent, represent the reality. However, it has not yet been justified how those equations can represent very complex debris flows and their interaction with shrubs. At present, there are fully physics-based multi-phase debris flow models (Pudasaini, 2012; Pudasaini & Mergili, 2019) that can be easily applied to the flow structure interaction simulation (Kafle et al., 2019; Kattel et al., 2018). These full and advanced mechanical models can also be used for the situation considered in the current study, enhancing the description and interpretation of physical phenomena. Therefore, subsequent studies should focus on the comprehensive effects of these factors. Another important aspect is to understand the erosion process and how the mass entrainment affects the flow dynamics and flow mobility. This can be achieved by applying the mechanical erosion model by Pudasaini and Krautblatter (2021).

Furthermore, vegetation is a crucial factor when assessing the possibility of mountain disasters, and it can regulate the conditions that contribute to disaster formation through mechanical and biological mechanisms (Rey & Labonne, 2015; Wang et al., 2017b). However, the effectiveness of vegetation is closely related to site conditions (Rey & Labonne, 2015; Wang et al., 2017b). For example, the comprehensive effect of vegetation on slopes is a balance between root reinforcement and increased slipping due to weight (Schmaltz & Mergili, 2018), and this balance depends on the slope. Moreover, vegetation is likely to increase the drag forces caused by wind and rainfall (Rengers et al., 2016). On slopes with relatively large slope gradients, vegetation will increase the instability of the soil. Even on steep slopes with thin soil layers, roots can cause cracks in the slope, increasing the probability of disasters under external disturbances. Therefore, in areas with good vegetation, the factors that have a significant effect on landslide and debris flow disasters (Xu et al., 2019), and how the values of these factors may affect the frequency of such events, have become key factors in landslide and debris flow forecasting and risk assessment studies.

It is crucial to further explore the relations between vegetation, environmental factors, and mountain disasters. Thus, further studies should aim to combine micro-level mechanisms to establish zoning maps for regional/global mountain disasters and dominant factors, evaluate the effectiveness of vegetation for disaster management comprehensively and objectively, and achieve in-depth analyses of regional disasters with respect to vegetation from processes to macro-scale patterns. This information will further clarify the positive and negative effects of vegetation in disaster management.

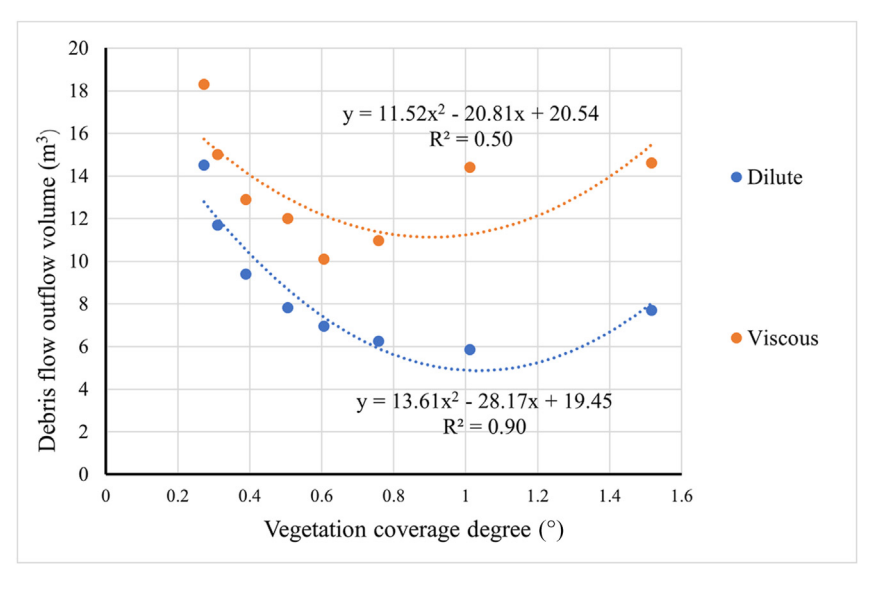


Fig. 18. Relation between the debris outflow volume and vegetation coverage.

5. Conclusions

The distribution patterns (row and stem spacings) of shrubs significantly affect the debris flow runoff reduction and sediment characteristics. Sixteen flume experiments were done to investigate the effect of shrubs within shrub filter strips on the movement of debris flows. For dilute debris flows, as the stem spacing increased, the bulk density reduction, flow reduction, flow velocity reduction, sediment interception, and particle size regulation capabilities of the shrub filter strip gradually decreased. As the row spacing increased, the flow velocity reduction rate and flow reduction rate gradually decreased. The bulk density reduction and sediment interception both increased at first and then decreased, and the particle size regulation remained approximately unchanged. For viscous debris flows, as the stem spacing increased the flow reduction, flow velocity reduction, and sediment interception effects gradually decreased, but the bulk density reduction and particle size regulation showed no noticeable changes. As the row spacing increased, the flow reduction, flow velocity reduction, and sediment interception all increased at first and then decreased, but the bulk density reduction and particle size regulation showed no noticeable changes.

Ecological engineering has become an increasingly important way of controlling landslides, debris flows, and other mountain disasters. In the current study, the sediment interception effects of different stem and row spacings for debris flows were explored. Preventing mountain disasters based on different perspectives is an extension of ecological engineering (such as root function and rainfall interception), which can help to promote the improvement and perfection of ecological engineering disaster controls. In the future, more attention should be given to the effects of multiple vegetation filter strips with different combinations of layout parameters. In addition, it would be desirable to measure the impact force on vegetation to understand the energy dissipation process, and numerical simulations could be used to explore more complex patterns.

Declaration of competing interest

The authors declare that they have no known competing financial interests or personal relationships that could have appeared to influence the work reported in this paper.

Acknowledgements

This research was supported by the National Science Fund for Distinguished Young Scholars of China (Grant No. 41925030), the National Natural Science Foundation of China (Grant No. 41790434), and the Youth science and technology fund of Institute of Mountain Hazards and Environment (IMHE Youth S&T Fund), Chinese Academy of Sciences (Grant No. SDS-QN-2108). The authors also would like to thank Editage for English language editing.

References

- Abu-Zreig, M., Rudra, R. P., Lalonde, M. N., Whiteley, H. R., & Kaushik, N. K. (2004). Experimental investigation of runoff reduction and sediment removal by vegetated filter strips. *Hydrological Processes*, 18, 2029–2037.
- Al-Zube, L., Sun, W., Robertson, D., & Cook, D. (2018). The elastic modulus for maize stems. Plant Methods, 14, 11.
- Bischetti, G. B., Dio, M. D. F., & Florineth, F. (2012). On the origin of soil bioengineering. *Landscape Research*, 39, 583–595.
- Burylo, M., Rey, F., Bochet, E., & Dutoit, T. (2012). Plant functional traits and species ability for sediment retention during concentrated flow erosion. *Plant and Soil*, 353, 135–144.
- Choi, C. E., Ng, C. W. W., Song, D., Kwan, J. H. S., Shiu, H. Y. K., Ho, K. K. S., & Koo, R. C. H. (2014). Flume investigation of landslide debris—resisting baffles. *Canadian Geotechnical Journal*, *51*(5), 540–553.
- Cui, Y., Jiang, Y., & Guo, C. (2019a). Investigation of the initiation of shallow failure in widely graded loose soil slopes considering interstitial flow and surface runoff. *Landslides*, 16, 815–828.

- Cui, Y., Li, J., Chen, A., Wu, J., Luo, Q., Rafay, L., He, J., Liu, Y., Wang, D., Lin, Y., & Wu, C. (2019b). Fractal dimensions of trapped sediment particle size distribution can reveal sediment retention ability of common plants in a dry-hot valley. *Catena*, 180, 252–262.
- Dalton, P. A., Smith, R. J., & Truong, P. N. V. (1996). Vetiver grass hedges for erosion control on a cropped flood plain: Hedge hydraulics. *Agricultural Water Management*, 31(1–2), 91–104.
- Durán Zuazo, D. V. H., & Rodríguez Pleguezuelo, C. R. (2008). Soil-erosion and runoff prevention by plant covers. A review (Vol. 28, pp. 65–86). Agronomy for Sustainable Development.
- Erktan, A., Cécillon, L., Roose, E., Frascaria-Lacoste, N., & Rey, F. (2013). Morphological diversity of plant barriers does not increase sediment retention in eroded marly gullies under ecological restoration. *Plant and Soil*, 370, 653–669.
- Evette, A., LaBonne, S., Rey, F., Liébault, F., Jancke, O., & Girel, J. (2009). History of bioengineering techniques for erosion control in rivers in western Europe. *Environmental Management*, 43, 972–984.
- Fu, S., Mu, H., Liu, B., Yu, X., Zhang, G., & Liu, Y. (2020). Effects on the plant stem arrangement on sediment transport capacity of croplands. *Land Degradation & Development*, 31, 1325–1334.
- Gonzalez-Ollauri, A., & Mickovski, S. B. (2017). Shallow landslides as drivers for slope ecosystem evolution and biophysical diversity. *Landslides*, 14, 1699–1714.
- Gregoretti, C., & Fontana, G. D. (2008). The triggering of debris flow due to channelbed failure in some alpine headwater basins of the dolomites: Analyses of critical runoff. *Hydrological Processes*, 22(13), 2248–2263.
- Gu, F., Ni, H., & Qi, D. (2007). Roughness coefficient for unsubmerged and submerged reed. Journal of Hydrodynamics, 19, 421–428.
- Guthrie, R. H., Hockin, A., Colquhoun, L., Nagy, T., Evans, S. G., & Ayles, C. (2009). An examination of controls on debris flow mobility: Evidence from coastal British Columbia. *Geomorphology*, 114(4), 601–613.
- Gyssels, G., Poesen, J., Bochet, E., & Li, Y. (2005). Impact of plant roots on the resistance of soils to erosion by water: A review. *Progress in Physical Geography*, 29(2), 189–217.
- Heller, V. (2011). Scale effects in physical hydraulic engineering models. *Journal of Hydraulic Research*, 49(3), 293–306.
- He, S., Wang, D., Chang, S., Fang, Y., & Lan, H. (2018). Effects of the morphology of sediment-transporting channels on the erosion and deposition of debris flows. *Environmental Earth Sciences*, 77, 544.
- He, S., Wang, D., Fang, Y., & Lan, H. (2017). Guidelines for integrating ecological and biological engineering technologies for control of severe erosion in mountainous areas—a case study of the Xiaojiang River Basin, China. *International* Soil and Water Conservation Research, 5, 335–344.
- Hong, Z. C., En, G. J., Jie, Z. M., Fei, W., & Tong, Z. (2016). Sediment deposition and overland flow hydraulics in simulated vegetative filter strips under varying vegetation covers. *Hydrological Processes*, 30, 163–175.
- Hübl, J., Suda, J., Proske, D., & Kaitna, R. (2009). Debris flow impact estimation. In Proceedings of the 11th international symposium on water management and hydraulic engineering (pp. 1–4). Ohrid, Mazedonien.
- Hu, X., Hu, K., Tang, J., You, Y., & Wu, C. (2019). Assessment of debris-flow potential dangers in the Jiuzhaigou Valley following the August 8, 2017, Jiuzhaigou earthquake, western China. *Engineering Geology*, 256, 57–66.
- Ishikawa, Y., Kawakami, S., Morimoto, C., & Mizuhara, K. (2003). Suppression of debris movement by forests and damage to forests by debris deposition. *Journal of Forest Research*, 8(1), 37–47.
- Isselin-Nondedeu, F., & Bédécarrats, A. (2007). Influence of alpine plants growing on steep slopes on sediment trapping and transport by runoff. *Catena*, 71, 330–339.
- Järvelä, J. (2002). Flow resistance of flexible and stiff vegetation: A flume study with natural plants. *Journal of Hydrology*, 269, 44–54.
- Kafle, J., Kattel, P., Mergili, M., Fischer, J., & Pudasaini, S. P. (2019). Dynamic response of submarine obstacles to two-phase landslide and tsunami impact on reservoirs. Acta Mechanica, 230, 3143–3169.
- Kattel, P., Kafle, J., Fischer, J.-T., Mergili, M., Tuladhar, B. M., & Pudasaini, S. P. (2018). Interaction of two-phase debris flow with obstacles. *Engineering Geology*, 242, 197–217.
- Kwan, J. S. H., Koo, R. C. H., & Ng, C. W. W. (2015). Landslide mobility analysis for design of multiple debris-resisting barriers. *Canadian Geotechnical Journal*, 52(9), 1345–1359.
- Lan, H., Wang, D., He, S., Fang, Y., Chen, W., Zhao, P., & Qi, Y. (2020). Experimental study on the effects of tree planting on slope stability. *Landslides*, 17, 1021–1035.
- Lee, K. H., Isenhart, T. M., Schultz, R. C., & Mickelson, S. K. (2000). Multispecies riparian buffers trap sediment and nutrients during rainfall simulations. *Journal of Environmental Quality*, 29, 1200–1205.
- Lin, Y., Chen, A., Yan, S., Rafay, L., Du, K., Wang, D., Ge, Y., & Li, J. (2019). Available soil nutrients and water content affect leaf nutrient concentrations and stoichiometry at different ages of Leucaena leucocephala forests in dry-hot valley. *Journal of Soils and Sediments*, 19, 511–521.
- Liu, D., Cui, Y., Guo, J., Yu, Z., Chan, D., & Lei, M. (2020). Investigating the effects of clay/sand content on depositional mechanisms of submarine debris flows through physical and numerical modeling. *Landslides*, 17, 1863–1880.
- Li, L., Yu, B., Zhu, Y., Chu, S., & Wu, Y. (2015). Topographical factors in the formation of gully-type debris flows in Longxi River catchment, Sichuan, China. *Environmental Earth Sciences*, 73(8), 4385–4398.
- Lobovský, L., Botia-Vera, E., Castellana, F., Mas-Soler, J., & Souto-Iglesias, A. (2014). Experimental investigation of dynamic pressure loads during dam break. *Journal of Fluids and Structures*, 48, 407–434.

- Malik, I., Tie, Y. B., Owczarek, P., Wistuba, M., & Pilorz, W. (2013). Human-planted alder trees as a protection against debris flow (A dendrochronological study from the Moxi Basin, Southwestern China). *Geochronometria*, 40(3), 208–216.
- Martinez-Raya, A., Zuazo, V. H. D., & Francia-Martinez, J. R. (2006). Soil Erosion and runoff response to plant-cover strips on semiarid slopes (SE Spain). *Land Degradation & elopementent, 17,* 1–11.
- May, C. (2002). Debris flows through different forest age classes in the central Oregon coast range. *Journal of the American Water Resources Association*, 38(4), 1097–1113.
- Mcardell, B. W., Bartelt, P., & Kowalski, J. (2007). Field observations of basal forces and fluid pore pressure in a debris flow. *Geophysical Research Letters*, 340(7).
- Mergili, M., Jaboyedoff, M., Pullarello, J., & Pudasaini, S. P. (2020). Back calculation of the 2017 Piz Cengalo—Bondo landslide cascade with r.avaflow: What we can do and what we can learn. Natural Hazards and Earth System Sciences, 20(2), 505–520.
- Michelini, T., Bettella, F., & D'Agostino, V. (2016). Field investigations of the interaction between debris flows and forest vegetation in two Alpine fans. Geomorphology, 279, 150–164.
- Mu, H., Yu, X., Fu, S., Yu, B., Liu, Y., & Zhang, G. (2019). Effect of stem basal cover on the sediment transport capacity of overland flows. *Geoderma*, 337, 384–393.
- Ng, C. W. W., Choi, C. E., Song, D., Kwan, J. H. S., Koo, R. C. H., Shiu, H. Y. K., & Ho, K. S. (2015). Physical modeling of baffles influence on landslide debris mobility. *Landslides*, 12(1), 1–18.
- Nilsson, C., Reidy, C. A., Dynesius, M., & Revenga, C. (2005). Fragmentation and flow regulation of the world's large river systems. Science, 308, 405–408.
- Pudasaini, S. P. (2012). A general two-phase debris flow model. *Journal of Geophysical Research Earth Surface*, 117, F03010.
- Pudasaini Shiva, P., & Fischer, J.-T. (2020). A mechanical model for phase separation in debris flow. *International Journal of Multiphase Flow, 129*, 103292.
- Pudasaini, S. P., & Mergili, M. (2019). A multi-phase mass flow model. *Journal of Geophysical Research Earth Surface*, 124, 2920—2942.
- Pudasaini, S. P., & Michaela, K. (2021). The mechanics of landslide mobility with erosion. *Nature Communications*, *12*, 6793.
- Reichenbach, P., Busca, C., Mondini, A. C., & Rossi, M. (2014). The influence of land use change on landslide susceptibility zonation: The briga catchment test site (Messina, Italy). *Environmental Management*, 54, 1372—1384.
- Rengers, F. K., Mcguire, L. A., Coe, J. A., Kean, J. W., Baum, R. L., Staley, D. M., & Godt, J. W. (2016). The influence of vegetation on debris-flow initiation during extreme rainfall in the northern Colorado Front Range. *Geology*, 44, 823–826.
- Rey, F., Bifulco, C., Bischetti, G. B., Bourrier, F., De Cesare, G., Florineth, F., Graf, F., Marden, M., Mickovski, S. B., Phillips, C., Peklo, K., Poesen, J., Polster, D., Preti, F., Rauch, H. P., Raymond, P., Sangalli, P., Tardio, G., & Stokes, A. (2019). Soil and water bioengineering: Practice and research needs for reconciling natural hazard control and ecological restoration. Science of the Total Environment, 648, 1210–1218.
- Rey, F., & Labonne, S. (2015). Resprout and survival of willow (salix) cuttings on bioengineering structures in actively eroding gullies in Marls in a mountainous

- mediterranean climate: A large-scale experiment in the francon catchment (southern alps, France). *Environmental Management*, 56, 971–983.
- Richet, J.-B., Ouvry, J.-F., & Saunier, M. (2017). The role of vegetative barriers such as fascines and dense shrub hedges in catchment management to reduce runoff and erosion effects: Experimental evidence of efficiency, and conditions of use. *Ecological Engineering*, 103, 455–469.
- Schmaltz, E. M., & Mergili, M. (2018). Integration of root systems into a GIS-based slip surface model: Computational experiments in a generic hillslope environment *Landslides*. 15, 1561–1575.
- Stokes, A., Douglas, G. B., Fourcaud, T., Giadrossich, F., Gillies, C., Hubble, T., Kim, J. H., Loades, K. W., Mao, Z., McIvor, I. R., Mickovski, S. B., Mitchell, S., Osman, N., Phillips, C., Poesen, J., Polster, D., Preti, F., Raymond, P., Rey, F., et al. (2014). Ecological mitigation of hillslope instability: Ten key issues facing researchers and practitioners. *Plant and Soil*, 377, 1–23.
- Sun, H., You, Y., & Liu, J. (2018). Experimental study on blocking and self-cleaning behaviors of beam dam in debris flow hazard mitigation. *International Journal* of Sediment Research. 33(4), 29–39.
- of Sediment Research, 33(4), 29–39.
 Sun, H., You, Y., Liu, J., Zhang, G., Feng, T., & Wang, D. (2021). Experimental study on discharge process regulation to debris flow with open-type check dams. Landslides, 18, 967–978.
- Tisserant, M., Janssen, P., Evette, A., González, E., & Poulin, M. (2020). Diversity and succession of riparian plant communities along riverbanks bioengineered for erosion control: A case study in the foothills of the alps and the Jura mountains. *Ecological Engineering*, 152(6), 105880.
- Vargas-Luna, A., Crosato, A., Calvani, G., & Uijttewaal, W. S. J. (2016). Representing plants as rigid cylinders in experiments and models. Advances in Water Resources, 93, 205–222.
- Wang, F., Chen, X., Chen, J., & You, Y. (2017). Experimental study on a debris-flow drainage channel with different types of energy dissipation baffles. *Engineering Geology*, 220, 43–51.
- Wang, W., Huai, W., Thompson, S., Peng, W., & Katul, G. G. (2018). Drag coefficient estimation using flume experiments in shallow non-uniform water flow within emergent vegetation during rainfall. *Ecological Indicators*, *92*, 367–378.
- Wang, S., Meng, X., Chen, G., Guo, P., Xiong, M., & Zeng, R. (2017b). Effects of vegetation on debris flow mitigation: A case study from Gansu province, China. *Geomorphology*, 282, 64–73.
- Xu, C., Yang, Z., Qian, W., Chen, S., Liu, X., Lin, W., Xiong, D., Jiang, M., Chang, C. T., Huang, J. C., & Yang, Y. (2019). Runoff and soil erosion responses to rainfall and vegetation cover under various afforestation management regimes in subtropical montane forest. *Land Degradation & Development*, 30, 1711–1724.
- Yin, Y., Cui, Y., Tang, Y., Liu, D., Lei, M., & Chan, D. (2021). Solid—fluid sequentially coupled simulation of internal erosion of soils due to seepage. *Granular Matter*, 23, 20.
- Zhang, S., Zhang, J., Liu, Y., Liu, Y., & Wang, Z. (2018). The effects of vegetation distribution pattern on overland flow. Water and Environment Journal, 32,
- Zhou, G., Hu, H. S., Song, D., Zhao, T., & Chen, X. Q. (2019). Experimental study on the regulation function of slit dam against debris flows. *Landslides*, *16*(1), 75–90.